Research Square

Preprints are preliminary reports that have not undergone peer review.
They should not be considered conclusive, used to inform clinical practice,
or referenced by the media as validated information.

# Synthesis and radiolabeling of a nitrofuran derivate with 18F for identification of areas of hypoxia in the tumor microenvironment

**Yasniel Babi Araujo** ( yasnielbabi1993@gmail.com )
IPEN: Instituto de Pesquisas Energeticas e Nucleares https://orcid.org/0009-0003-6601-3672
**Maria Ângela Pepe Carneiro**
IPEN: Instituto de Pesquisas Energeticas e Nucleares
**Fabio Fernando Alves da Silva**
IPEN: Instituto de Pesquisas Energeticas e Nucleares
**André Luis Lapolli**
IPEN: Instituto de Pesquisas Energeticas e Nucleares
**Emerson Soares Bernardes**
IPEN: Instituto de Pesquisas Energeticas e Nucleares

**Research Article**

**Keywords:** (E)-1-(4-[18F]-fluorophenyl)-3-(5-nitrofuran-2-yl)prop-2-en-1-one, [18F]FNFP, hypoxia, Positron Emission Tomography, 5-nitrofuran, oxygen-mimetic chemical sensitizers

**Posted Date:** February 16th, 2024

**DOI:** https://doi.org/10.21203/rs.3.rs-3918714/v1

**License:** This work is licensed under a Creative Commons Attribution 4.0 International License.
Read Full License

# Abstract

## Background

Positron Emission Tomography (PET) is a non-invasive molecular imaging technique widely known for studying hypoxia mostly employing 2-nitroimidazole-based radiotracers. These probes are based on the oxygen-mimetic chemical sensitizers of hypoxic cells developed for cancer therapy during the 1970s. 5-nitrofuran derivates are more electron affinic than nitroimidazoles, therefore, higher specificity for hypoxic regions is expected for the formers, and new radiotracer probes bearing a 5-nitrofuran ring could be used for imaging hypoxia.

## Results

A nitrofuran-based radiotracer for detection of hypoxic areas in the tumor microenvironment, (E)-1-(4-[$^{18}$F]-fluorophenyl)-3-(5-nitrofuran-2-yl)prop-2-en-1-one, baptized as [$^{18}$F]FNFP, was obtained. Two copper-mediated nucleophilic radiofluorination procedures were tested and compared using the same pinacol-derived aryl boronic ester precursor: method 1, using $K_{222}/K_2CO_3$ and $[Cu(OTf)_2(py)_4]$ afforded the product in 56 ± 8% (n = 5) RCY after HPLC analysis of the crude reaction mixture; method 2: an azeotropic drying-free [$^{18}$F]-labelling procedure, using $Cu(OTf)_2$ as [$^{18}$F]-elution agent and copper source, yielded [$^{18}$F]FNFP in 88 ± 4% (n = 5) RCY. Method 2 was chosen as the standard for the synthesis of the radiotracer, obtaining the product with an overall radiochemical yield of 38,4 ± 3% (n = 5), high radiochemical purity (> 99%), total synthesis time of 85 minutes and a molar activity of 41.56 GBq/μmol. [$^{18}$F]FNFP was found to be stable in serum and Phosphate-buffered saline for up to 6h, and lipophilicity measurements concluded that it is more hydrophilic than [$^{18}$F]FMISO ($\log10P$=2.6), with $\log10P$=1.05.

**Conclusion**:

The first nitrofuran-based radiotracer to be used as a PET hypoxia imaging agent was efficiently radiolabeled with 18F. In vitro and in vivo studies are being lined up to compare [18F]FNFP with [18F]FMISO and [18F]FAZA.


# Background

Hypoxia, one of the hallmarks of cancer (1, 2), is a condition where oxygen levels are below the normal physiological concentration in tissues that results from an imbalance between oxygen supply and oxygen consumption. Solid tumors are likely to develop hypoxic regions and are associated with poor prognosis, an increased risk of invasion and metastasis, and resistance to chemo and radiation therapies (1–4).

Tumor hypoxia has been studied using several different techniques such as extrinsic (e.g., pimonidazole) and intrinsic (e.g., carbonic anhydrase IX, CAIX) biomarkers; blood oxygen level-dependent (BOLD) and tissue oxygen level-dependent (TOLD); molecular imaging through Single Photon Emission Computed Tomography (SPECT) and Positron Emission Tomography (PET), magnetic resonance imaging (MRI) and

oxygen electrodes (5), often referred as the “gold standard” (6). Among them, SPECT and PET as non-invasive modalities rely on radiolabeled probes that are selectively accumulated within cells under hypoxic conditions after undergoing enzymatic-mediated reductions. Many of these SPECT/PET-used radiolabeled probes are based on nitroaromatic hypoxic-cell sensitizers, oxygen-mimetic compounds developed to improve the radiosensitivity of hypoxic cells within solid tumors in radiotherapy (7). In the 1970s nitroaromatic compounds such as the antibiotic and antibacterial agents nitrofurans (e.g. nitrofurazone, nifurtimox, nitrofurantoin nifuroxime) and specially nitroimidazoles were identified as sensitizers; Misonidazole and Metronidazole (Fig. 1) were two of the earliest developed ones, with the former been more effective due to a higher electron affinity as measured by one-electron reduction potential ($E_7^1$, first electron reduction potential at neutral pH), which is a key factor in their efficacy (8). Subsequent attempts to demonstrate hypoxic cell sensitization by these compounds *in vivo* unfortunately failed in most cases due to neurotoxicity, compromised stability and water low water solubility in case of nitrofurans, and in case of misonidazole the maximum clinical doses that could be achieved fell well short of those required for maximum sensitizing effectiveness (9, 10).

Those same properties that allow radiosensitizers to accumulate under hypoxic conditions are used to determine the location of hypoxic cells and measure tumor hypoxia, approach that was first carried out with $^{14}$C-radiolabelled misonidazole (11) and was the breakthrough that led to PET and SPECT imaging probes for detection of hypoxia. In this regard, [$^{18}$F]fluoromisonidazole ([$^{18}$F]FMISO, 1*H*-1-(3-[$^{18}$F]fluoro-2-hydroxypropyl)-2-nitroimidazole) first synthetized in 1986 (12) is the most widely used hypoxia imaging radiopharmaceutical, but its high lipophilicity causes slow tracer accumulation, slow plasma clearance, and low tumor-to-background contrast. Most of the other radiotracers developed to solve [$^{18}$F]FMISO pharmacokinetic issues, such as [$^{18}$F]Fluoroazomycin Arabinoside ([$^{18}$F]FAZA), [18F]Fluoroerythronitroimidazole ([$^{18}$F]FETNIM), [$^{18}$F]fluoroetanidazole ([$^{18}$F]FETA) and [$^{18}$F]-Flortanidazole ([$^{18}$F]FHX4), rely on the 2-nitroimidazole moiety (Fig. 1), or even 4- or 5-nitroimidazole derivates have been tested (13, 14). The literature shows that each radiotracer for detection of hypoxic regions in tumors has its strengths and weaknesses depending on the study and the information required a different one can be put forward in every situation.

The nitroimidazole moiety is not considered to be essential for an “ideal” nitroaromatic radiosensitizer and therefore neither for a hypoxia imaging agent. This compound should have high membrane permeability (measured by partition coefficient) to ensure a feasible cell-membrane penetration and accumulation in the target tissue, but also has to be sufficiently soluble in water to deliver appreciable amounts of the drug (15). Additionally, the $E_7^1$ must be between that of $O_2$ (-155 mV) and the cytochromes, which transport these reducing equivalents (approximately − 450 mV) (15): a compound with a $E_7^1$ close to oxygen would be too electron affinic therefore toxic, and a weakly-affinic one would lose its sensitivity and selectivity for hypoxia. According to Martin Brown, Paul Workman (16) the best balance between toxicity and sensitivity occurs for radiosensitizers approximately at -390 mV, which is where the $E_7^1$ of most 2-nitroimidazoles is (-380 to -400 mV range). However, the actual $E_7^1$ values depend on the side chain and the inductive effects of the substituents present on it.

Based on the idea that, in general, the therapeutic benefit or efficiency of hypoxic cell sensitizers could be improved by increasing radiosensitizing potency, fact that could be achieved by raising the redox potential of the nitroheterocycle, Naylor, M A et al. (17) synthetized a group of 5-nitrofuran derivates in order to test their efficiency as sensitizers based on the premise that these nitroaromatic compounds are slightly more electron affinic than 2-nitroimidazoles. The 5-nitrofurans investigated showed high radiosensitizing activity *in vitro* and all of them were more efficient sensitizers than misonidazole, with $E_7^1$ values ranging from − 211 to approximately − 327 mV. The major issue was their toxicity, at least 1 order of magnitude greater than are the toxicities of similar nitroimidazoles (17).

A radiotracer bearing a 5-nitrofuran moiety instead of a nitroimidazole one for imaging hypoxia could be an interesting solution to finding the “ideal” imaging agent. Theoretically, the higher reduction potential of the nitrofuran ring would not only allow this probe to maintain its selectivity for hypoxia, but this selectivity would be, at least, equal to that of 2-nitroimidazole derivatives. Then its side chain will domain its lipophilicity and pharmacokinetic properties.

In this work, and for the first time, a nitrofuran-based radiotracer (E)-1-(4-[$^{18}$F]fluorophenyl)-3-(5-nitrofuran-2-yl)prop-2-en-1-one, baptized as [$^{18}$F]FNFP was radiolabeled with fluorine-18 in order to be tested as a hypoxia imaging agent. The chalcone-based structure used would increase even more its electron affinity as result of electron delocalization throughout the whole structure, idea supported by several authors (18, 19).

## Results

# Chemical synthesis

The synthesis path to obtain (E)-1-(4-fluorophenyl)-3-(5-nitrofuran-2-yl)prop-2-en-1-one, [$^{19}$F]FNFP (compound 4), and (E)-(4-(3-(5-nitrofuran-2-yl)acryloyl)phenyl)boronic acid pinacol ester, [$^{18}$F]FNFP precursor (compound 6) is shown in scheme 1.

First, nitration of furfural in acetic anhydride in the presence of $HNO_3$ and catalytic $H_2SO_4$ yielded 5-nitro-2-furaldehyde diacetate (compound 2) as a white crystalline solid in 60% yield after recrystallization from ethanol. The 1,1-diacetate (acylal) protecting group was removed in refluxing acetonitrile in the presence of catalytic $SnCl_2xH_2O$ to yield 5-nitro-2-furaldehyde (compound 3) in 90% yield as a yellow solid after column chromatography in silica gel. Claisen-Schmidt condensation of 5-nitrofuraldehyde and 4-fluoroacetophenone in acidic media yielded cold standard (E)-1-(4-fluorophenyl)-3-(5-nitrofuran-2-yl)prop-2-en-1-one (compound 4) as yellow needles in 75% yield after recrystallization from ethanol.

The synthesis of (E)-(4-(3-(5-nitrofuran-2-yl)acryloyl)phenyl)boronic acid pinacol ester, compound 6, started with a metal-free borylation reaction using 4-aminoacetophenone as starting material to obtain 4-acetyl phenylboronic acid pinacol ester (compound 5) as a white-off crystalline solid in 65% yield after flash chromatography in silica gel. Finally, another acidic Claisen-Schmidt condensation now between 5-

nitro-2-furaldehyde and 4-acetyl phenylboronic acid pinacol ester yielded (E)-(4-(3-(5-nitrofuran-2-yl)acryloyl)phenyl)boronic acid pinacol ester as yellow needles in 72% yield after recrystallization from ethanol.

# Radiochemistry

Two different procedures were studied for the synthesis of [$^{18}$F]FNFP. Scheme 2 shows the reaction details:

Following the radiosynthesis procedure described in method 1 in the experimental section, [$^{18}$F]FNFP was obtained with a radiochemical yield (RCY) of 56 ± 8% (n = 5) after HPLC analysis of the crude reaction mixture using [$Cu(OTf)_2(py)_4$] as copper source. “Cold” standard [$^{19}$F]FNFP was used as a reference for the comparison during quality control of the radioactive peak during the radio-HPLC run (Fig. 2) shows a representative chromatogram of a crude reaction mixture sample.

Now following the radiosynthesis procedure described in method 2 (scheme 2), [$^{18}$F]FNFP was obtained with a radiochemical yield of 88 ± 4 (n = 5) after radio-HPLC analysis of the crude reaction mixture, also using [$^{19}$F]FNFP “cold” standard as reference (Fig. 3).

Comparing both methods 1 and 2 for the synthesis of [$^{18}$F]FNFP, the results showed that radiochemical yields are higher for method 2. Then, this protocol was chosen as the standard for the synthesis of our radiotracer.

After the synthesis following method 2, semipreparative HPLC purification afforded > 99% radiochemically pure [$^{18}$F]FNFP (Fig. 4), with an overall radiochemical yield of 38,4 ± 3% (n = 5), total synthesis time of 85 minutes and a molar activity of 41.56 GBq/μmol.

### In vitro stability

The stability of the new radiopharmaceutical [$^{18}$F]FNFP in 0.1 mol/L PBS at pH = 7.2 and in serum was evaluated for a period of up to 6 hours. Aliquots were taken immediately after the synthesis, 1, 3 and 6 hours after it, and the radiochemical purity of the compound was assessed by HPLC following the same conditions as described earlier for its quality control.

As demonstrated in Fig. 5, no significant metabolites derived from [$^{18}$F]FNFP were observed after 6h of incubation either in PBS or serum.

# Determination of partition coefficient

The logarithm of [$^{18}$F]FNFP partition coefficient calculated according to the methodology described was $\log_{10}P$=1.05 ± 0.06 (n = 7).

# Discussion

Historically, nitroimidazole-based compounds have been used as radiotracers for detection of hypoxia based on their previous introduction as radiosensitizers of hypoxic cells and their good pharmacokinetic properties, specially 2-nitroimidazole ones, due to their higher electron affinity compared to 4- and 5-nitroimidazoles derivates. In this regard, [$^{18}$F]FMISO is the most widely used radiopharmaceutical for imaging tumor hypoxia using PET (20), but because of its high lipophilicity pharmacokinetic issues are associated to it. Second and third-generation radiotracers have been developed (20), and even some of them have undergone preclinical trials in the past recent years (21). Nevertheless, none of these radiotracers have shown to be vastly superior to [$^{18}$F]FMISO so the latter remains as the radiolabeled imaging agent that has been more used for investigating tumor hypoxia.

Nitrofurans, as one of the most important and studied nitroaromatic compounds, were also tested as sensitizers with promising results related to their higher sensitizing potency (attributable to their higher reduction potential) compared to 2-nitroimidazole derivates. The issue associated with them was their toxicity, so more attention was paid to nitroimidazoles. The mechanism of action of these nitroaromatic compounds involves metabolic changes related to the nitro group accepting electrons from reducing enzymes (nitroreductases) hence generating intermediates that react with DNA to exert toxic and mutagenic effects (22, 23). These sensitizers get into intracellular space by diffusion and under hypoxic condition the process described above takes place, but under normal oxygen concentrations the compound is re-oxidized back to the original one and diffuses out of the cell (20).

In this work, the first use of a lipophilic nitrofuran-based radiotracer ([$^{18}$F]-FNFP) labeled with $^{18}$F intended to become a hypoxia imaging agent is described. In order to improve its electron affinity, a side chain based on a chalcone structure was built according to the following ideas: A) in a study reported by Valdez et al. (2009) (18), where the authors synthetized several 5-nitroimidazole derivates and tested their antimicrobial activity against *Giardia lamblia*, compounds having olefins with a conjugated bridge connecting the nitroheterocycle and a substituted phenyl or heterocyclic ring showed greatly increased antigiardial activity without toxicity (Fig. 6, A). Electrochemical studies carried out in that work (determination of the half-wave potential of the initial one-electron transfer by cyclic voltammetry) showed that the electron delocalization in these compounds was associated with an easier redox activation and reduction, therefore correlated with greater antigiardial activity. B) In another work published by Tawari, Nilesh R. et al. (2010) (24) the authors synthetized a series of potent nitrofuran-based antitubercular agents coupling electronegative α,β-unsaturated carbonyl bridge to the nitrofuran ring and substituted phenyl or heterocyclic rings (Fig. 6, B). Based on density functional theory (DFT) and computational studies, these compounds were selected as strong candidates to become antitubercular agents because all of them possessed localized negative potential regions near the oxygen atom of the carbonyl group and both the oxygen atoms of the nitro group that extend laterally to the furan ring oxygen, due to electron delocalization, an idea that was previously reported by the same authors in an attempt to highlight structural features required for potent antitubercular activity (19). One more time, the electron delocalization was linked to an improved electron affinity and therefore good antitubercular activity and low toxicity.

Two different radiofluorination procedures were followed to efficiently obtain [$^{18}$F]FNFP. The “traditional” radiofluorination of pinacol-derived aryl boronic esters using $K_{222}/K_2CO_3$ and $[Cu(OTf)_2(py)_4]$ first reported by the Gouverneur group (25) afforded [$^{18}$F]FNFP in a much lower radiochemical yield (according to a crude reaction mixture analysis) than the azeotropic drying-free [$^{18}$F]-labelling of aryl boronic acids and pinacol esters reported by Lahdenpohja, Salla Orvokki et al. (26). Many issues associated with the use of high quantities of base ($K_2CO_3$) in radiofluorination reactions have been reported in the past few years (27, 28). Low radiochemical yields and the impossibility of using base-sensitive precursors limit the scope of the late-stage radiofluorination approach, especially for radiofluorination of aryl boronic esters and derivates because of the high temperatures (110–130ºC) necessary for this copper-mediated $^{18}$F-fluorination to be carried out. In the second method used for the synthesis of [$^{18}$F]FNFP only copper II triflate (a cheaper alternative to $[Cu(OTf)_2(py)_4]$) was used as [$^{18}$F]-elution agent from the anion exchange cartridge, also diminishing the total number of steps compared to method 1.

Chalcone and its derivates (and in our case here FNFP), α,β-unsaturated precursors of flavonoid and isoflavonoid-based compounds, either natural or synthetic exhibit various biological activities, such as anti-inflammatory, analgesic, antioxidant, antibacterial, antifungal, anti-tuberculosis, antimalarial, antiviral, and antitumor (29). These compounds’ conjugated structure is characterized by a high delocalization of the electrons and a low redox potential that provide remarkable chances of undergoing electron transfer reactions (30). The presence of the α,β-unsaturated carbonyl functional group, that acts as a potential Michael acceptor, allows the chalcone (or its derivate) molecule to interact with sulfhydryl of cysteine residue or other thiol groups (30, 31). Stability tests executed with [$^{18}$F]FNFP showed that this probe is stable both in serum and Phosphate-buffered saline (PBS), but further *in vivo* tests need to be carried out in order to evaluate [$^{18}$F]FNFP’s possible binding to proteins due to the possible reaction of Michael donors with the α,β-unsaturated carbonyl group present on its structure.

Lipophilicity measurement afforded a $\log_{10}P$ value of 1.05 for [$^{18}$F]FNFP, which is lower than that of [$^{18}$F]FMISO ($\log_{10}P$=2.6) (32) and the same for another 2-nitroimidazole-based hypoxia imaging probe developed by our group in another work, N-(4-[$^{18}$F]fluorobenzyl)-2-(2-nitro-1H-imidazol-1-yl)-acetamide [$^{18}$F]FBNA (33).

Now it is necessary to evaluate the uptake of this probe under hypoxic/normoxic conditions. Our group is already planning those experiments, and also a comparison *in vitro* and *in vivo* with two other stablished radiotracers for studying hypoxia, [$^{18}$F]FMISO and [$^{18}$F]FAZA.

# Methods

# General methods and instruments

Reagents and solvents were purchased from Sigma Aldrich LTDA, Brazil, and used without further purification. Reactions were monitored by thin-layer chromatography (TLC) using silica gel 60 UV-254 pre-coated silica gel plates from MERCK®. Detection was by means of a UV lamp. Flash column chromatography was performed on 300–400 mesh silica gel. Nuclear Magnetic Resonance (NMR), one-dimensional and two-dimensional analyzes of $^{1}H$ and $^{13}C$ nuclei were acquired with Bruker Avance spectrometers (USA) model DPX-300 MHz and DRX-600 MHZ and Bruker Ultra-Shield 300 spectrometer FT-NMR. Chemical shifts are given in ppm referenced to internal standards (s = singlet, singlet, d = doublet, t = triplet, m = multiplet); the coupling constant (J), described in Hertz (Hz); and the number of hydrogens deduced from the relative integral.

Infrared (IR) spectra were obtained on a Fourier Transform Infrared Spectrometer (FTIR) Fourier Transform Infrared Spectrophotometer, IRTracer-100 (Shimadzu), in the spectral region from 4000 to 500 $cm^{-1}$. High resolution mass spectroscopy (HRMS) data were obtained on a Bruker Daltonics mass spectrometer, model microOTOF-Q II - ESI-Qq-TOF and 4000 QTRAP AB SCIEX. Melting points were determined on a Buchi M-560 melting point apparatus BUCHI Brazil Ltda

Measurement of [$^{18}F$] radioactivity was performed using a Carpintec dose calibrator (CRC-15R, New Jersey, USA). The Agilent High Performance Liquid Chromatography (HPLC) system (USA) was used for quality control of compounds labeled with [$^{18}F$]. The system is equipped with a model 1260 quaternary pump, a model 1260 UV absorbance detector and a radioactivity detector (Raytest, Germany). Agilent Chem Station software was used to operate Agilent HPLC systems. The HPLC equipment with UV and radioactivity detector, as well as the column used for analysis (ZORBAX Eclipse Plus C18 Analytical 4.6 x 250 mm, 5 µm) are from Agilent Technologies, Brazil.

# Chemical synthesis

### Synthesis of 5-nitro-2-furaldehyde diacetate

Furfural was nitrated following the procedure reported by Taimoory, S. Maryamdokht et al. with some modifications (34). Briefly, Acetic anhydride (180 mL) was placed in a dried 500-mL three-necked, round-bottomed flask equipped with a mechanical stirrer and a thermometer, and afterwards the mixture was then cooled to -10ºC in a benzyl alcohol/dry ice bath. 17.2 mL of concentrated $HNO_3$ and 0.15 mL of concentrated $H_2SO_4$ were mixed in a small beaker, and this solution was slowly and carefully added into the chilled acetic anhydride while stirring between − 10ºC and − 5ºC. Afterwards, 20.8 mL (0.251 mol) of freshly distilled furfural was added dropwise over 20 minutes into the cold acid mixture with stirring at the same temperature, and the resulting solution was left to stir for 1 h between − 10ºC and − 5ºC. After this time 160 mL of water were added, and the mixture was left to stir at room temperature for 30 min, over which a white precipitate formed. A 10% NaOH solution was added to the mixture until the pH rose to 2.5–2.7, and it was warmed on a water bath at 55ºC for 1h. The mixture was poured into crushed ice, stirred for 10 min and the white precipitate formed filtered, washed with water, recrystallized twice from ethanol, and air-dried to provide 36.63 g of the product as a white crystalline solid in 60% yield. **$^{1}H$ NMR**

(300 MHz, Chloroform-d) δ 7.73 (s, 1H), 7.30 (d, J = 3.6 Hz, 1H), 6.75 (d, J = 3.6 Hz, 1H), 2.19 (s, 6H) (Supplementary file 1). **m.p.** 90–91 ºC.

### Synthesis of 5-nitro-2-furaldehyde

5-nitro-2-furaldehyde was obtained following a procedure reported by Mohammadpoor-Baltork, I. and Aliyan, H. (35). In short, to a solution of 5-Nitro-2-furaldehyde diacetate (4.864 g, 20 mmol) in acetonitrile (100 mL), was added $SnCl_2.2H_20$ (902.52 mg, 4 mmol, 20% mol) and the clear mixture was refluxed for 1h (turned dark after 20 min of reaction) when TLC (100% toluene) indicated completion. The solvent was evaporated, and the residue was purified by flash column chromatography eluting with chloroform to give 2.54 g of 5-nitro-2- furaldehyde as a yellow solid in 90% yield. **$^1$H-NMR** (600 MHz, Chloroform-d) δ 9.85 (s, 1H), 7.44 (dd, J = 3.8, 0.4 Hz, 1H), 7.38 (d, J = 3.8 Hz, 1H) (Supplementary file 2). **m.p.** 38-38.7ºC.

### Synthesis of (E)-1-(4-fluorophenyl)-3-(5-nitrofuran-2-yl)prop-2-en-1-one, [$^{19}$F]-FNFP

Following the methodology reported by Tawari, Nilesh R et al. (24), 5-nitro-2-furaldehyde (988 mg, 7 mmol) was dissolved in 10 mL of glacial acetic acid at room temperature. 400 µL of concentrated sulfuric acid and 4-fluoroacetophenone (7 mmol, 846 µL) were added in sequence, and the mixture was stirred at room temperature overnight. Ice-cold water (50 mL) was added, the solid was recovered by filtration and washed carefully with ice cold ethanol. The product was then recrystallized from ethanol to yield 1.37 g of (E)-1-(4-fluorophenyl)-3-(5-nitrofuran- 2-yl)prop-2-en-1-one as yellow needles in 75% yield. **$^1$H-NMR** (600 MHz, DMSO-*d*6) δ 8.26–8.20 (m, 2H), 7.89 (d, *J* = 15.6 Hz, 1H), 7.83 (d, *J* = 3.9 Hz, 1H), 7.61 (d, *J* = 15.6 Hz, 1H), 7.47 (d, *J* = 3.9 Hz, 1H), 7.45–7.41 (m, 2H) (Supplementary file 3). **m.p.** 183–184ºC.

### Synthesis of 4-acetyl phenylboronic acid pinacol ester

Following the procedure reported by Mo, Fanyang et al. (36), 4-aminobenzophenone (1.352 g, 10 mmol), bis(pinacolato)diboron (2.667 g, 10.5 mmol, 1.05 equiv.) and benzoyl peroxide (20.4 mg, 0.08426 mmol, 2% mol) were weighted in a 50 mL round-bottom flask. To this mixture, anhydrous acetonitrile (15 mL) was added, and then tert-butyl nitrite (1.785 mL, 15 mmol, 1.5 equiv.) in 5 mL of anhydrous acetonitrile was added dropwise at room temperature with stirring. The resulting mixture was stirred at room temperature overnight, and the solvent was removed under reduced pressure. The residue was purified by flash column chromatography eluting with hexanes/ethyl acetate 1/50 to 1/20 to give 1.6 g of 4-acetyl phenylboronic acid pinacol ester as a white-off crystalline solid in 65% yield. **$^1$H-NMR** (600 MHz, Chloroform-d) δ 7.85–7.77 (m, 4H), 2.51 (s, 3H), 1.26 (s, 12H) (Supplementary file 4). **m.p.** 59–60ºC.

**Synthesis of (E)-(4-(3-(5-nitrofuran-2-yl)acryloyl)phenyl)boronic acid pinacol ester**: 5-nitro-2-furaldehyde (168 mg, 1.2 mmol) was dissolved in 1.5 mL of glacial acetic acid at room temperature. 120 µL of concentrated sulfuric acid and 4-acetyl phenylboronic acid pinacol ester (295.3 mg, 1.2 mmol) were added in sequence, and the mixture was stirred at room temperature overnight. Ice-cold water (5 mL) was added, the solid was recovered by filtration and washed carefully with ice cold ethanol. The product was then recrystallized from ethanol to yield 319 mg of (E)-(4-(3-(5- nitrofuran-2-yl)acryloyl)phenyl)boronic

acid pinacol as yellow needles in 72% yield. **$^{1}$H-NMR** (600 MHz, DMSO-*d*6) δ 8.12–8.10 (m, 2H), 7.89–7.84 (m, 3H), 7.83 (d, *J* = 3.9 Hz, 1H), 7.62 (d, *J* = 15.6 Hz, 1H), 7.47 (d, *J* = 3.9 Hz, 1H), 1.33 (s, 12H) (Supplementary file 5). **$^{13}$C-NMR DEPTQ** (151 MHz, DMSO) δ 153.60, 152.50, 139.30, 135.30, 129.41, 128.28, 125.31, 118.52, 115.26, 84.62, 25.15 (Supplementary file 6). **m.p.** 170–171ºC. **ESI-mass spectrometry**. $[M + Na]^{+}$=392,1274 expected MW = 369,18 g/mol (Supplementary file 7). **Infrared spectra**: (= C-H) aromatic 3118 $cm^{-1}$; (C-H) 2929 $cm^{-1}$; carbonyl stretching vibration for the enone (= C-C = O) 1661 $cm^{-1}$; N–O asymmetric stretch 1479 $cm^{-1}$, N–O symmetric stretch 1365 $cm^{-1}$ (Supplementary file 8).

# Radiochemistry

No-carrier-added $[^{18}F]F^{-}$ was produced by $^{18}O(p,n)^{18}F$ reaction in an 18-MeV cyclotron (IBA, Belgium). Sep-Pak Light QMA cartridges (Waters, Brazil) were pre-conditioned using two different methods: 1) 10 mL of 0.5 M $K_2CO_3$ solution, followed by 20 mL of Milli-Q water and purged with 5 mL of air; 2) 10 mL of 0.5M potassium triflate (KOTf), followed by 20 mL of Milli-Q water and purged with 5 mL of air.

# Radiosynthesis of (E)-1-(4-[$^{18}$F]fluorophenyl)-3-(5-nitrofuran-2-yl)prop-2-en-1-one [$^{18}$F]FNFP

Two different methodologies were studied to prepare [$^{18}$F]FNFP manually.

Method 1, following the procedure reported by Tredwell, Matthew et al. (25). In short, the fluoride ion $[^{18}F]^{-}$ solution was trapped in an anionic Sep Pak light QMA cartridge, previously conditioned with $K_2CO_3$ 0.5 M and water, and the $[^{18}F]^{-}$ was then eluted into the reaction vial with a mixture of $K_2CO_3$ (2.8 mg; 20 µmol) and Kryptofix 2.2.2 (15 mg; 40 µmol) in 1 mL of acetonitrile/water (8:2). Then, the solution was subjected to three cycles of azeotropic distillation with anhydrous acetonitrile (1mL) at 100°C under a nitrogen flow. Afterwards, (E)-(4-(3-(5-nitrofuran-2-yl)acryloyl)phenyl)boronic acid pinacol ester (4.8 mg, 13 µmol) in 150 µL of anhydrous DMA and $[Cu(OTf)_2(py)_4]$ (8.8 mg, 13 µmol) in 150 µL of DMA were added and the resulting solution was stirred at 120ºC for 20 min under air, quenched with water (300 µL) and an aliquot was removed for analysis by radio-HPLC to calculate the RCY and identify the product, respectively.

Method 2, according to a procedure reported by Lahdenpohja, S.O., Rajala, N.A., Rajander, J. *et al.* (26). Succinctly, the fluoride ion $[^{18}F]^{-}$ solution (80–100 mCi, approximately 1–2 mL) was diluted in 8–10 mL of fresh miliQ water in a flask. This solution was taken up in a 20 mL syringe and passed through a pre-conditioned anionic QMA cartridge, previously conditioned with KOTf 0.5 M and water. The cartridge was slowly washed with 5 mL of anhydrous DMA, and the $[^{18}F]^{-}$ was then eluted with a solution of $Cu(OTf)_2$ (34.7 mg, 96 µmol) in anhydrous DMA (0.5 mL) into the reaction vial already containing (E)-(4-(3-(5-nitrofuran-2-yl)acryloyl)phenyl)boronic acid pinacol ester (5.5 mg, 15 µmol) diluted in 50 µL of anhydrous DMA and 50 µL of anhydrous pyridine. The QMA cartridge was washed with 0.5 mL of anhydrous DMA into the reaction vial, giving a total volume of 1.1 mL, and the resulting blue solution was stirred at 120ºC

for 20 min under air. The reaction was quenched with water (500 µL) and an aliquot was removed for analysis by radio-HPLC to calculate the RCY and identify the product, respectively.

After HPLC identification of the product, [$^{18}$F]FNFP crude reaction mixture was then taken up in water (20 mL) and passed through a pre-conditioned C18 plus cartridge. The product was then eluted from the C18 with 1 mL of ethanol and purified by semipreparative HPLC using MiliQ water (0.1% trifluoroacetic acid), channel A, and acetonitrile, channel B, with a gradient run using 10%-100% of B in 20 minutes, with a flux of 3 mL/min, retention time 14–15 min.

# Quality control

Aliquots of the final formulation of labeled [$^{18}$F]-FNFP and standard (cold) compound [$^{19}$F]-FNFP were analyzed by HPLC to determine chemical purity, radiochemical purity, molar activity and confirm chemical identity. The compounds were analyzed with the following analysis conditions:

[$^{18}$F]-FNFP and [$^{19}$F]-FNFP: Stationary phase: ZORBAX Eclipse Plus C18 Analytical column 4.6 x 250 mm (5 µm). Mobile phase: Solvent (A) Milli Q water 0.1%TFA, Solvent (B) 100% Acetonitrile. Run: Gradient, 90%(A) : 10% B to 100% B for 20 min. Injection: 20 µCi for [$^{18}$F]-FNFP and 5 µg for [$^{19}$F]-FNFP, Flow: 1 mL/min. Wavelength: 350 nm.

# Determination of molar activity

Molar activity was determined by a building a standard curve from the HPLC trace of the corresponding fluorinated “cold” standard compound [$^{19}$F]-FNFP [Y axis = UV area, X axis = mole number (µmol)] (Supplementary files 9 and 10). After semipreparative HPLC purification, 20 µCi (0.74 MBq) of [$^{18}$F]-FNFP was injected onto the HPLC and the UV area overlapping with the radio peak was recorded and the standard curve was used to calculate mole number. Dividing the product decay corrected activity by the mole number gives the molar activity in GBq/µmol.

### In vitro stability

[$^{18}$F]-FNFP stability was assessed at room temperature in 0.1 mol/L PBS at pH = 7.2. The samples had an activity of 3.7 MBq (1 mCi) of [$^{18}$F]-FNFP in a final volume of 1 mL. The stability of the compound was monitored for 6 hours (immediately after the synthesis, 1, 3 and 6 hours after synthesis) and the results analyzed by HPLC as described in the previous section. The stability of the final formulation was also evaluated in Nude serum. In this case, an aliquot of 800 µL (1mCi) was added to 500 µL of freshly separated serum, and the mixture was incubated at 37°C for up to 6 hours. Aliquots of 100 µL were withdrawn at different times (immediately after the synthesis, 1, 3 and 6 hours after synthesis) and 100 µL of acetonitrile were added to precipitate serum proteins. Then the solution was centrifuged (5000 rpm, for 10 min) and the supernatant was analyzed by HPLC.

# Determination of lipophilicity

The lipophilicity of [$^{18}$F]FNFP was determined by measuring the octanol-water partition coefficient as described by Barthel, H., Wilson, H., Collingridge, D. *et al.* (37) with some modifications.. Shortly, 80 – 100 µCi (2.96–3.70 MBq) of [$^{18}$F]-FNFP were dissolved in distilled $H_2O$ in a 10 mL falcon tube to a final volume of 0.5 mL and 0.5 mL of octan-1-ol (Sigma-Aldrich Brasil LTDA) was added. The tube was capped and shaken vigorously for 2–3 min and subsequently centrifuged for 30 min (5000 rpm; Rotina 35R, Hettich Zentrifugen, Tuttlingen, Germany). Aliquots (100 µL) of the resulting top layer (representing [$^{18}$F]-FNFP dissolved in octanol), and bottom layer ([$^{18}$F]-FNFP dissolved in $H_2O$) were taken and the radioactivity in these samples was measured using a dose calibrator, CRC – 10BC, Carpintec Inc., USA. Eight octanol–$H_2O$ mixtures were analyzed (n = 8), and the octanol –water partition coefficient was calculated by dividing the octanol-containing radioactivity by the water-containing radioactivity.

# Conclusions

In this work, the first nitrofuran-based imaging probe to be used as PET hypoxia imaging agent was synthetized and radiolabeled with $^{18}$F. An azeotropic drying-free copper-mediated radiofluorination of a pinacol-derived aryl boronic ester precursor allowed the radiosynthesis to be carried out in 85 minutes obtaining the product [$^{18}$F]FNFP with a radiochemical yield of 38,4 ± 3% (n = 5). Subsequent *in vitro* cellular uptake studies under hypoxic conditions and *in vivo* in tumor bearing mice are already being planned up, also including a comparison of [$^{18}$F]FNFP with [$^{18}$F]FMISO and [$^{18}$F]FAZA.

# Abbreviations

$B_2pin_2$: bis(pinacolato)diboron; BPO: benzoyl peroxide; DMA: dimethyl acetamide; [$^{18}$F]$F^-$: $^{18}$F-fluoride; HPLC: high performance liquid chromatography; $K_{222}$: Kryptofix 2.2.2; $K_2CO_3$: potassium carbonate; m/z: mass-to-charge ratio; MeCN: acetonitrile; PET: positron emission tomography; RCY: radiochemical yield; QMA: quaternary methyl ammonium; SPECT: Single Photon Emission Computed Tomography; TFA: trifluoroacetic acid; TLC: thin layer chromatography; $[Cu(OTf)_2(py)_4]$: tetrakis(pyridine)copper(ii) triflate.

# Declarations

### Ethics approval and consent to participate

Not applicable

### Consent for publication

Not applicable

### Competing interests

The authors declare that they have no competing interests

### Availability of data and material

Contact the corresponding author


### Funding

This research was funded by CNPq – Brazilian Federal Agency for Support and Evaluation of Graduate Education within the Ministry of Education of Brazil - Finance Code 142245/2018-6.


### Authors' contributions

All the authors read and approved the final manuscript. YBA performed the experiments and contributed to the design and analysis of data, reviewed the literature, and wrote the manuscript. MAPC, FFAS and ALL contributed to the experiments performed and help revising the manuscript. Methodology, YBA, ALL and ESB. Funding acquisition, ESB.


### Acknowledgments

The authors would like to thank to the staff of Cyclotron Facilities and Radiopharmacy Center at IPEN, São Paulo, Brazil.


## References


1. Hanahan D, & Weinberg, R. A. Hallmarks of cancer: the next generation. Cell. 2011;144(5):646–74.
2. Tímár J, Sebestyén A., Kopper L., Dankó T. Hypoxia Signaling in Cancer: From Basics to Clinical Practice Pathology and Oncology Research 2021;27.
3. Abou Khouzam R, Brodaczewska, K., Filipiak, A., Zeinelabdin, N. A., Buart, S., Szczylik, C., Kieda, C., & Chouaib, S. Tumor Hypoxia Regulates Immune Escape/Invasion: Influence on Angiogenesis and Potential Impact of Hypoxic Biomarkers on Cancer Therapies. Frontiers in Immunology 2021;11.
4. Ruan K, Song, G., & Ouyang, G. Role of hypoxia in the hallmarks of human cancer. Journal of cellular biochemistry. 2009;107(6):1053–62.
5. Flood A, Wood V, Swartz H. Comparing the Effectiveness of Methods to Measure Oxygen in Tissues for Prognosis and Treatment of Cancer. 9232016. p. 113-20.
6. L. Olive JPBCA-PP. Measuring Hypoxia in Solid Tumours&Is There a Gold Standard? Acta Oncologica. 2001;40(8):917-23.
7. Fowler JF, Adams GE, Denekamp J. Radiosensitizers of hypoxic cells in solid tumours. Cancer Treatment Reviews. 1976;3(4):227-56.
8. Adams GE, Flockhart IR, Smithen CE, Stratford IJ, Wardman P, Watts ME. Electron-Affinic Sensitization: VII. A Correlation between Structures, One-Electron Reduction Potentials, and Efficiencies of Nitroimidazoles as Hypoxic Cell Radiosensitizers. Radiation Research. 1976;67(1):9-20.

9. Martin Brown J. Clinical perspectives for the use of new hypoxic cell sensitizers. International Journal of Radiation Oncology*Biology*Physics. 1982;8(9):1491-7.
10. Dische S. Chemical sensitizers for hypoxic cells: A decade of experience in clinical radiotherapy. Radiotherapy and Oncology. 1985;3(2):97-115.
11. Chapman J, Franko, A. & Sharplin, J. . Br J Cancer. A marker for hypoxic cells in tumours with potential clinical applicability. British Journal of Cancer. 1981;43:546–50.
12. Jerabek PA, Patrick TB, Kilbourn MR, Dischino DD, Welch MJ. Synthesis and biodistribution of 18F-labeled fluoronitroimidazoles: Potential in vivo markers of hypoxic tissue. International Journal of Radiation Applications and Instrumentation Part A Applied Radiation and Isotopes. 1986;37(7):599-605.
13. Nguyen AT, Kim H-K. Recent Advances of 68Ga-Labeled PET Radiotracers with Nitroimidazole in the Diagnosis of Hypoxia Tumors. International Journal of Molecular Sciences [Internet]. 2023; 24(13).
14. Heiss D, Sorensen GA, Takasawa M, Ramez, Moustafa R, Mrcp, et al., editors. Section Editors: Wolf-Applications of Nitroimidazole in Vivo Hypoxia Imaging in Ischemic Stroke.
15. Kumar P, Bacchu V, Wiebe LI. The Chemistry and Radiochemistry of Hypoxia-Specific, Radiohalogenated Nitroaromatic Imaging Probes. Seminars in Nuclear Medicine. 2015;45(2):122-35.
16. Brown JM, Workman P. Partition Coefficient as a Guide to the Development of Radiosensitizers Which Are Less Toxic Than Misonidazole. Radiation Research. 1980;82(1):171-90.
17. Naylor MA, Stephens, M. A., Cole, S., Threadgill, M. D., Stratford, I. J., O'Neill, P., Fielden, E. M., & Adams, G. E. Synthesis and evaluation of novel electrophilic nitrofuran carboxamides and carboxylates as radiosensitizers and bioreductively activated cytotoxins. Journal of Medicinal Chemistry. 1990;33(9):2508–13.
18. Valdez CA, Tripp JC, Miyamoto Y, Kalisiak J, Hruz P, Andersen YS, et al. Synthesis and Electrochemistry of 2-Ethenyl and 2-Ethanyl Derivatives of 5-Nitroimidazole and Antimicrobial Activity against Giardia lamblia. Journal of Medicinal Chemistry. 2009;52(13):4038-53.
19. Tawari NR, Degani MS. Pharmacophore Modeling and Density Functional Theory Analysis for A Series of Nitroimidazole Compounds with Antitubercular Activity. Chemical Biology & Drug Design. 2011;78(3):408-17.
20. Fleming IN, Manavaki, R., Blower, P. J., West, C., Williams, K. J., Harris, A. L., Domarkas, J., Lord, S., Baldry, C., & Gilbert, F. J. Imaging tumour hypoxia with positron emission tomography. British journal of cancer. 2015;112(2):238–50.
21. Mees G, Dierckx, R., Vangestel, C., & Van de Wiele, C. Molecular imaging of hypoxia with radiolabelled agents. European Journal of Nuclear Medicine and Molecular Imaging. 2009;36(10):1674–86.
22. Priyanka D. KR. Nitroaromatics as hypoxic cell radiosensitizers: A 2D-QSAR approach to explore structural features contributing to radiosensitization effectiveness. European Journal of Medicinal Chemistry Reports. 2022;4.
23. Patterson S, & Wyllie, S. Nitro drugs for the treatment of trypanosomatid diseases: past, present, and future prospects. Trends in parasitology. 2014;30(6):289–98.

24. Tawari NR, Bairwa R, Ray MK, Rajan MGR, Degani MS. Design, synthesis, and biological evaluation of 4-(5-nitrofuran-2-yl)prop-2-en-1-one derivatives as potent antitubercular agents. Bioorganic & Medicinal Chemistry Letters. 2010;20(21):6175-8.
25. Tredwell M, Preshlock SM, Taylor NJ, Gruber S, Huiban M, Passchier J, et al. A General Copper-Mediated Nucleophilic 18F Fluorination of Arenes. Angewandte Chemie International Edition. 2014;53(30):7751-5.
26. Lahdenpohja SO, Rajala NA, Rajander J, Kirjavainen AK. Fast and efficient copper-mediated 18F-fluorination of arylstannanes, aryl boronic acids, and aryl boronic esters without azeotropic drying. EJNMMI Radiopharmacy and Chemistry. 2019;4(1):28.
27. Haveman LYF, Vugts DJ, Windhorst AD. State of the art procedures towards reactive [18F]fluoride in PET tracer synthesis. EJNMMI Radiopharmacy and Chemistry. 2023;8(1):28.
28. Mossine A, Brooks A, Ichiishi N, Makaravage K, Sanford M, Scott P. Development of Customized [18F]Fluoride Elution Techniques for the Enhancement of Copper-Mediated Late-Stage Radiofluorination. Scientific Reports. 2017;7.
29. Mohamed MFA, Abuo-Rahma GE-DA. Molecular targets and anticancer activity of quinoline–chalcone hybrids: literature review. RSC Advances. 2020;10:31139 - 55.
30. Maydt D, De Spirt S, Muschelknautz C, Stahl W, Müller TJJ. Chemical reactivity and biological activity of chalcones and other α,β-unsaturated carbonyl compounds. Xenobiotica. 2013;43(8):711-8.
31. Zhuang C, Zhang W, Sheng C, Zhang W, Xing C, Miao Z. Chalcone: A Privileged Structure in Medicinal Chemistry. Chemical Reviews. 2017;117(12):7762-810.
32. Piert M, Machulla, H. J., Picchio, M., Reischl, G., Ziegler, S., Kumar, P., Wester, H. J., Beck, R., McEwan, A. J., Wiebe, L. I., & Schwaiger, M. Hypoxia-specific tumor imaging with 18F-fluoroazomycin arabinoside. Journal of Nuclear Medicine. 2005;46(1):106–13.
33. Nario AP, Woodfield, J., Dos Santos, S. N., Bergman, C., Wuest, M., Araújo, Y. B., Lapolli, A. L., West, F. G., Wuest, F., & Bernardes, E. S. Synthesis of a 2-nitroimidazole derivative N-(4-[18F]fluorobenzyl)-2-(2-nitro-1H-imidazol-1-yl)-acetamide ([18 F]FBNA) as PET radiotracer for imaging tumor hypoxia. EJNMMI radiopharmacy and chemistry. 2022;7(1).
34. Taimoory SM, Sadraei, S. I., Fayoumi, R. A., Nasri, S., Revington, M., & Trant, J. F. Preparation and Characterization of a Small Library of Thermally-Labile End-Caps for Variable-Temperature Triggering of Self-Immolative Polymers. The Journal of Organic Chemistry. 2018;83(8):4427–40.
35. Mohammadpoor-Baltork I, Alivan, H.;. Efficient and selective deprotection of aryl aldehyde diacetates catalyzed by tin(II) chloride dihydrate. Indian Journal of Chemistry, Section B: Organic Chemistry Including Medicinal Chemistry. 1999;38B(10):1223-5.
36. Mo F, Jiang Y, Qiu D, Zhang Y, Wang J. Direct Conversion of Arylamines to Pinacol Boronates: A Metal-Free Borylation Process. Angewandte Chemie International Edition. 2010;49(10):1846-9.
37. Barthel H, Wilson H, Collingridge DR, Brown G, Osman S, Luthra SK, et al. In vivo evaluation of [18F]fluoroetanidazole as a new marker for imaging tumour hypoxia with positron emission tomography. British Journal of Cancer. 2004;90(11):2232-42.

# Scheme

Scheme 1 and 2 are available in the Supplementary Files section.

# Figures

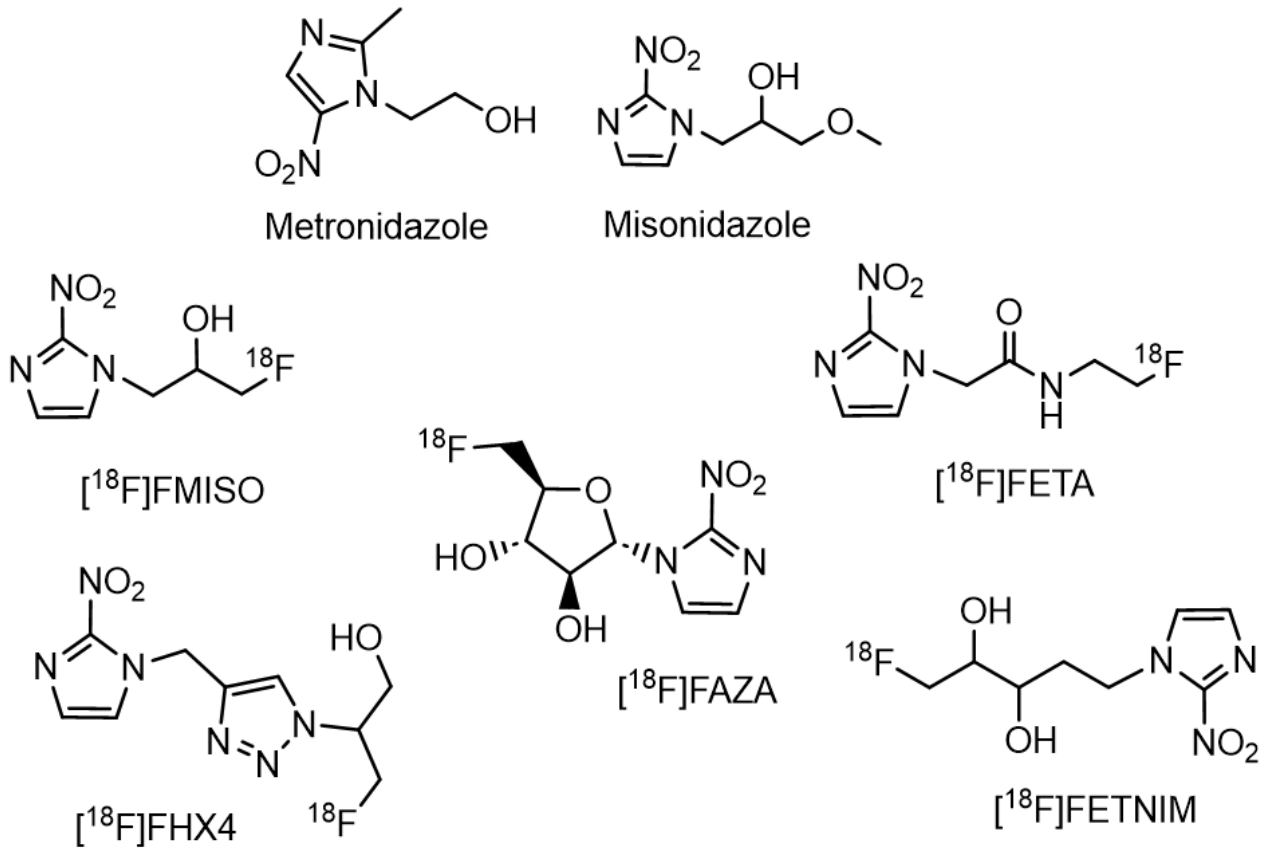


**Figure 1**

Misonidazole and Metronidazole, two of the first nitroimidazole-based sensitizers studied for radiosensitization of hypoxic cells. [$^{18}$F]FMISO, [$^{18}$F]FAZA, [$^{18}$F]FETNIM, [$^{18}$F]FETA and [$^{18}$F]FHX4 some of the most important 2-nitroimidazole-based PET hypoxic imaging agents.

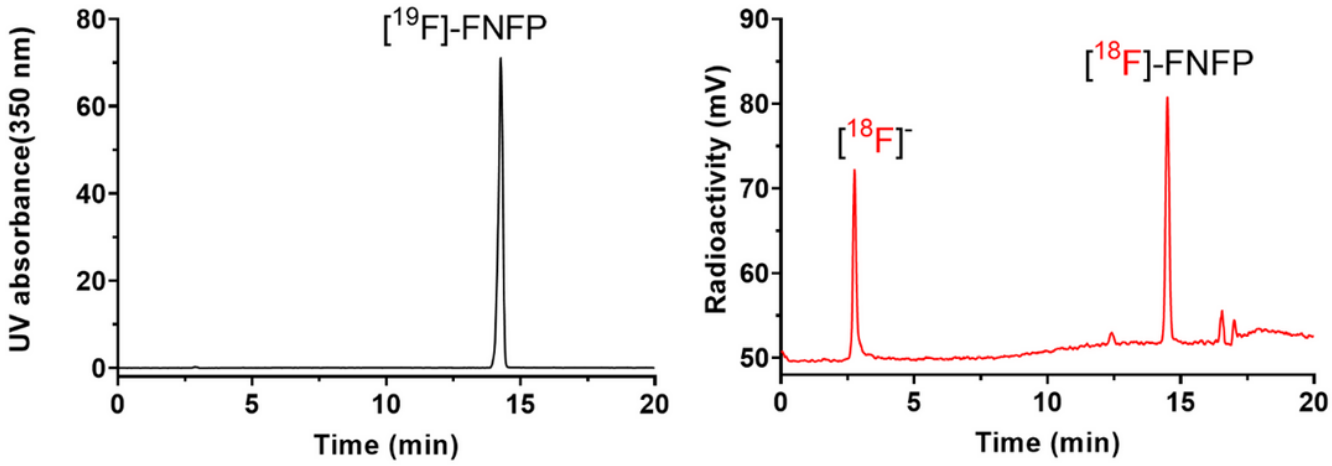


## Figure 2

On the left, HPLC chromatogram of “cold” standard [$^{19}$F]FNFP at retention time 14,261 min, λ=350 nm. On the right, crude reaction mixture chromatogram showing free [$^{18}$F]$^{-}$ fluoride and [$^{18}$F]FNFP at 14,357 min retention time.

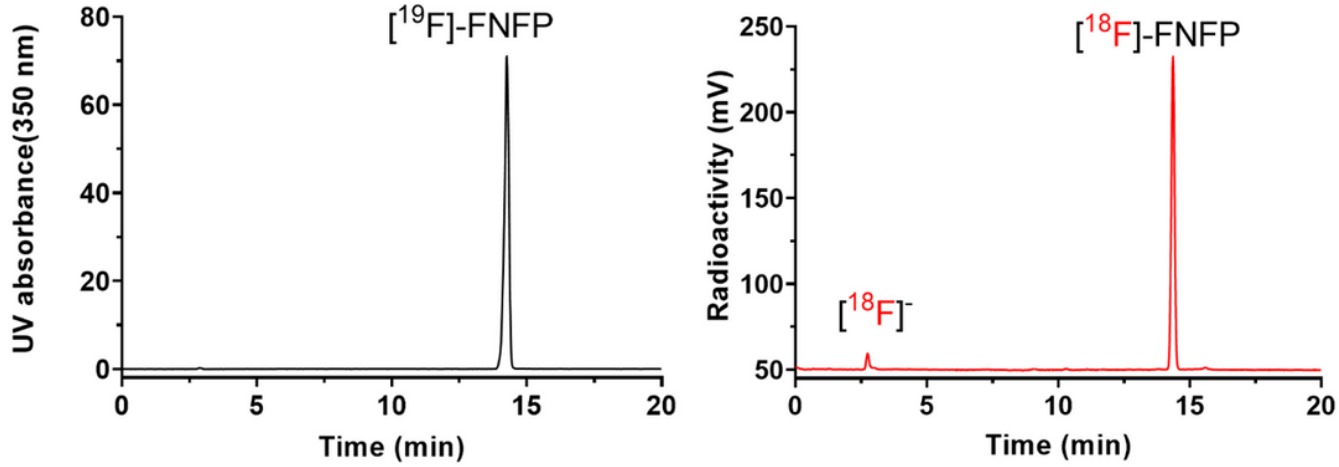


## Figure 3

On the left, HPLC chromatogram of “cold” standard [$^{19}$F]FNFP at retention time 14,261 min, λ=350 nm. On the right, crude reaction mixture chromatogram showing free [$^{18}$F]$^{-}$ fluoride and [$^{18}$F]FNFP at 14,388 min retention time.

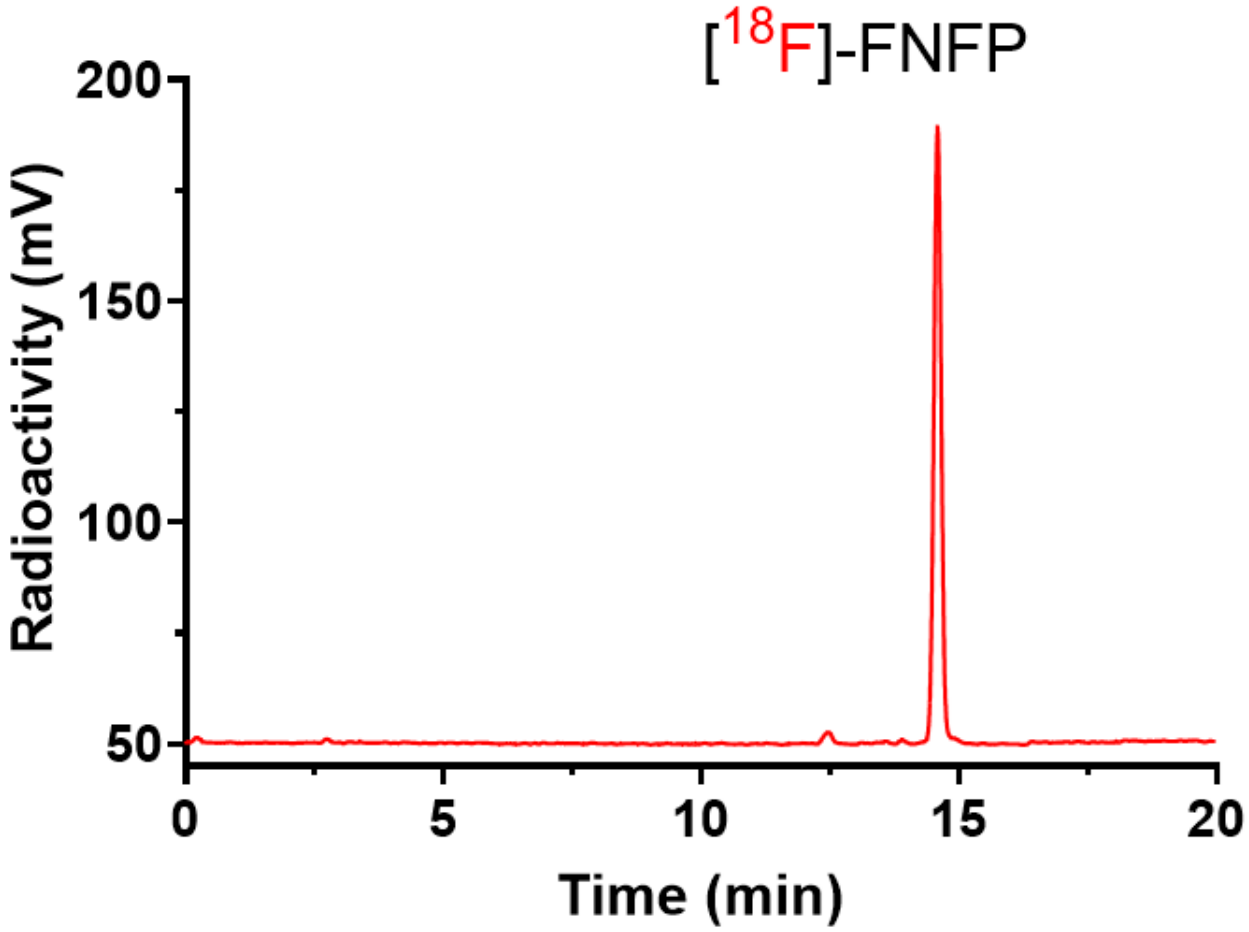


**Figure 4**

[$^{18}$F]FNFP (retention time 14,261 min) after semipreparative HPLC purification.

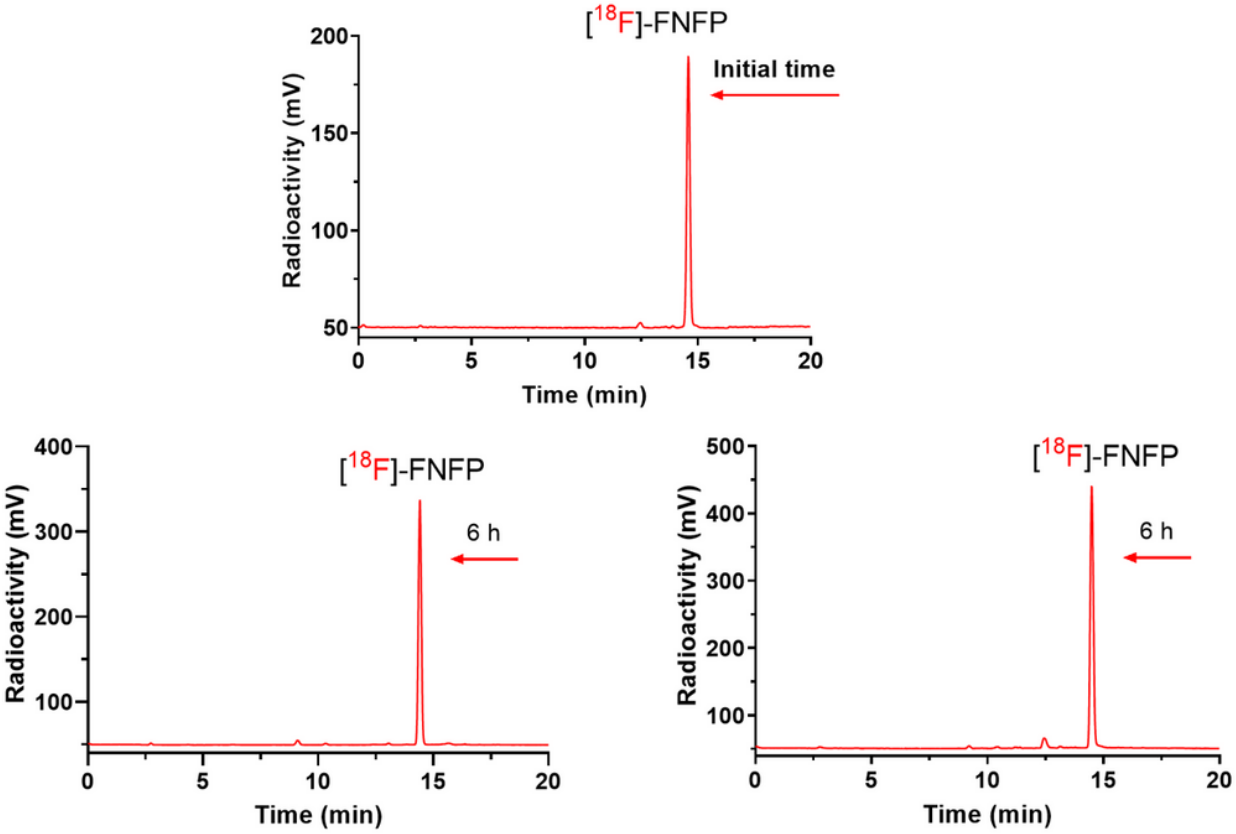


**Figure 5**

Radioactivity profile obtained by radio-HPLC of the stability of [$^{18}$F]FNFP (retention time 14,2 min) after 6 hours in 0.1 mol/L PBS at pH=7.2 (right bottom) and in serum (left bottom). Above, [$^{18}$F]FNFP at the beginning of the stability test (initial time).

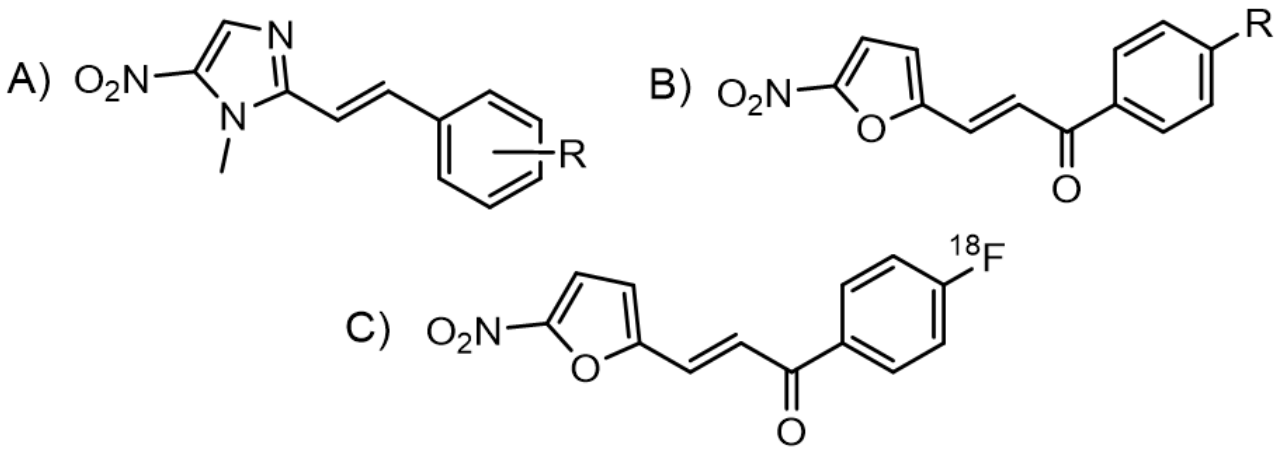


**Figure 6**

A) Compounds obtained by Valdez et al. bearing olefins with a conjugated bridge connecting a nitroimidazole ring and a substituted phenyl or heterocyclic ring (18). B) Compounds synthetized by Tawari, Nilesh R. et al. having a furan moiety and α,β-unsaturated carbonyl bridge (24). C) (E)-1-(4-[$^{18}$F]fluorophenyl)-3-(5-nitrofuran-2-yl)prop-2-en-1-one, [$^{18}$F]FNFP obtained in this work.

## Supplementary Files

This is a list of supplementary files associated with this preprint. Click to download.

- Supplementaryfile1.tiff
- Supplementaryfile10.tif
- Supplementaryfile2.tiff
- Supplementaryfile3.tiff
- Supplementaryfile4.tiff
- Supplementaryfile5.tiff
- Supplementaryfile6.tiff
- Supplementaryfile7.pdf
- Supplementaryfile8.tif
- Supplementaryfile9.docx
- scheme1.png
- scheme2.png